

## Supporting Information

### Harnessing solvent effect to integrate alkylamine into metal-organic frameworks for exceptionally high CO<sub>2</sub> uptake

Hao Li,<sup>a</sup> Kecheng Wang,<sup>a</sup> Zhigang Hu,<sup>b</sup> Ying-Pin Chen,<sup>ac</sup> Wolfgang Verdegaal,<sup>d</sup> Dan Zhao,<sup>\*b</sup> and Hong-Cai Zhou<sup>\*ac</sup>

<sup>a</sup> *Department of Chemistry, Texas A&M University, College Station, Texas 77842-3012, USA.*

<sup>b</sup> *Department of Chemical and Biomolecular Engineering, National University of Singapore, 4 Engineering Drive 4, 117585, Singapore.*

<sup>c</sup> *Department of Materials Science and Engineering, Texas A&M University, College Station, Texas 77843, USA.*

<sup>d</sup> *Profusa, Inc. 345 Allerton Ave. South San Francisco, California 94080, USA.*

\*To whom correspondence should be addressed:

Prof. Hong-Cai Zhou [zhou@chem.tamu.edu](mailto:zhou@chem.tamu.edu);

Prof. Dan Zhao [chezhao@nus.edu.sg](mailto:chezhao@nus.edu.sg)

## Section 1. Chemicals

Chromium (III) nitrate nonahydrate ( $\text{Cr}(\text{NO}_3)_3 \cdot 9\text{H}_2\text{O}$ ), terephthalic acid ( $\text{H}_2\text{BDC}$ ), hydrofluoric acid 48-51 wt% (HF), ethanol (EtOH), ammonium fluoride ( $\text{NH}_4\text{F}$ ), acetone, cyclohexane (CH), dichloromethane (DCM), diethylenetriamine (DETA), tris(2-aminoethyl)amine (TAEA), 40% w/w sodium deuterioxide ( $\text{NaOD}$ ) solution in deuterium oxide ( $\text{D}_2\text{O}$ ) solution (99.5%) were purchased from VWR. All commercial chemicals were used without further purification unless otherwise mentioned.

## Section 2. Instruments

Powder X-ray diffraction (PXRD) was carried out with a BRUKER D8-Focus Bragg-Brentano X-ray Powder Diffractometer equipped with a Cu sealed tube ( $\lambda = 1.54178 \text{ \AA}$ ) at 40 kV and 40 mA. Images and analyses of SEM/EDX were taken by FEI Quanta 600 FE-SEM. The Quanta 600 FEG is a field emission scanning electron microscope capable of generating and collecting high-resolution and low-vacuum images. It is equipped with a motorized x-y-z-tilt-rotate stage, providing the following movements: x = y = 150 mm (motorized); z = 65 mm (motorized); Tilt +70 degrees to -5 degrees (motorized); Source: Field emission gun assembly with Schottky emitter source. Voltage: 200 V to 30 kV. Beam Current: >100 nA. Equipment associated with the Quanta 600 includes: conventional Everhart-Thornley detector, back-scattered electron detector, IR-CCD chamber camera, Oxford EDX system equipped with X-ray mapping and digital imaging, HKL/Oxford EBSD system incl. geological phase database for phase ID, Gatan panchromatic cathodoluminescence detector with RGB filters and a Zyvex S100 nanomanipulator.  $\text{N}_2$  and  $\text{CO}_2$  sorption isotherms were measured using a Micromeritics ASAP 2020 system at various temperatures. Nuclear magnetic resonance (NMR) analysis was taken by Mercury 300 (300 MHz routine walkup H/C system). Thermogravimetric analysis (TGA) was performed on Mettler Toledo TGA/DSC (DSC = Differential Scanning Calorimetry) 1 Star System. The TGA instrument is coupled with a mass spectrometer (OmniStar ThermoStar GSD320 Gas Analysis System) for the analysis of gas species.

## Section 3. Preparation of MIL-101(Cr)

A mixture of  $\text{Cr}(\text{NO}_3)_3 \cdot 9\text{H}_2\text{O}$  (400 mg, 1.0 mmol), terephthalic acid ( $\text{H}_2\text{BDC}$ , 166 mg, 1.0 mmol), deionized water (4.75 mL), and HF (48-51 wt%, 20  $\mu\text{L}$ ) was added into a 5 mL Teflon-lined stainless-steel autoclave and heated at 200 °C for 8 h.<sup>1</sup> After the mixture was cooled to room temperature (RT), the as-synthesized solid was washed successively with 100 mL 95:5 EtOH: $\text{H}_2\text{O}$  (v/v) solution at 80 °C for 24 h, 90 mL 30 mmol/L  $\text{NH}_4\text{F}$  solution at 70 °C for 24 h, and 67 mL deionized water at 90 °C for 3h. The resulting solid was further washed with acetone for three times, desiccated in air, and activated at 160 °C under vacuum for 12 h prior to further use.

#### Section 4. Pore size distributions of alkylamine-modified MIL-101(Cr)

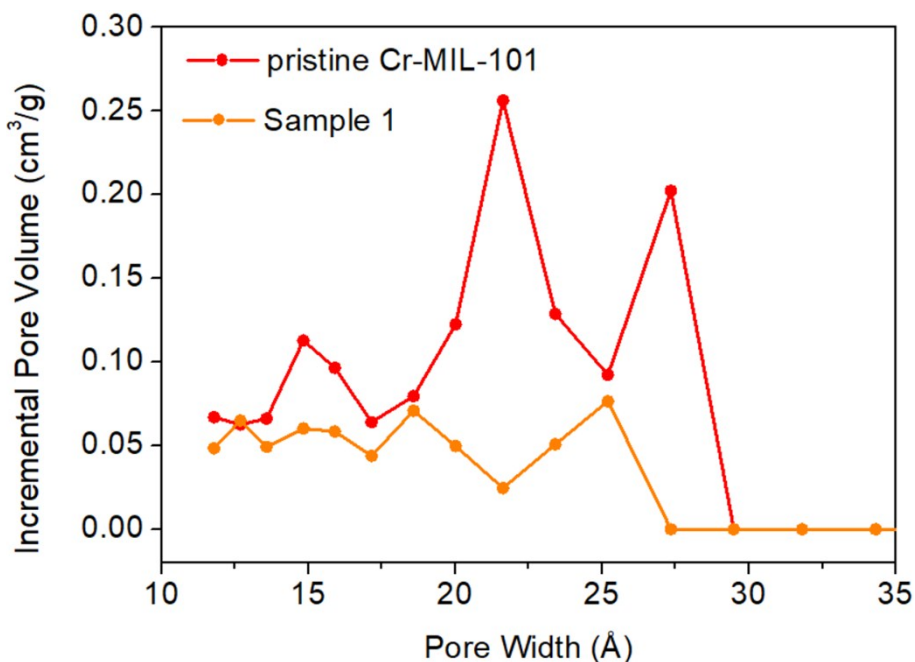


**Figure S1.** Pore size distribution of **Sample 1** in comparison with that of the pristine MIL-101(Cr). The total pore volume in **Sample 1** ( $\leq 272.71 \text{ \AA}$ ) is determined to be  $0.67651 \text{ cm}^3/\text{g}$ .

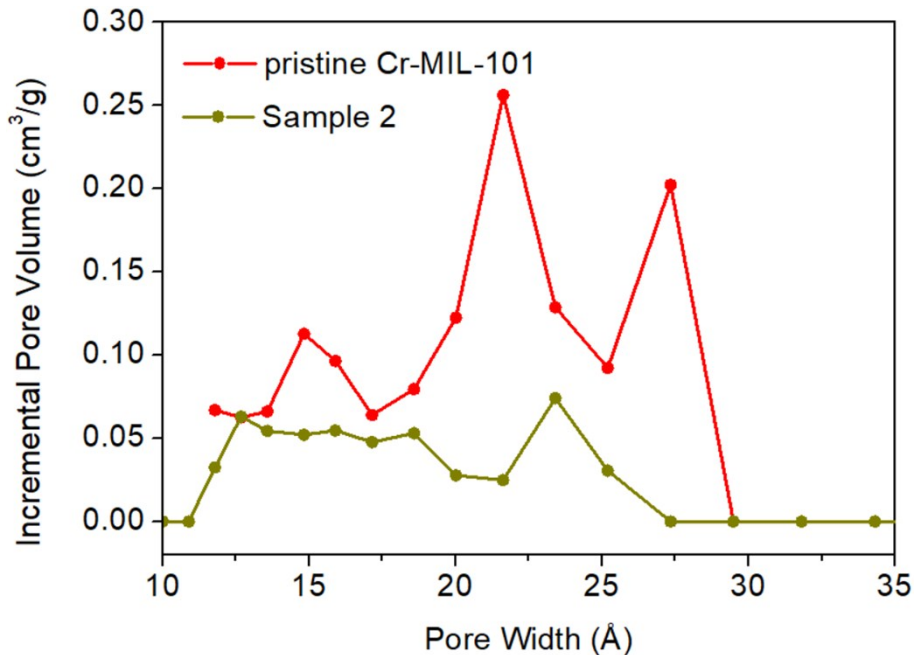


**Figure S2.** Pore size distribution of **Sample 2** in comparison with that of the pristine MIL-101(Cr). The total pore volume in **Sample 2** ( $\leq 272.71 \text{ \AA}$ ) is determined to be  $0.57573 \text{ cm}^3/\text{g}$ .

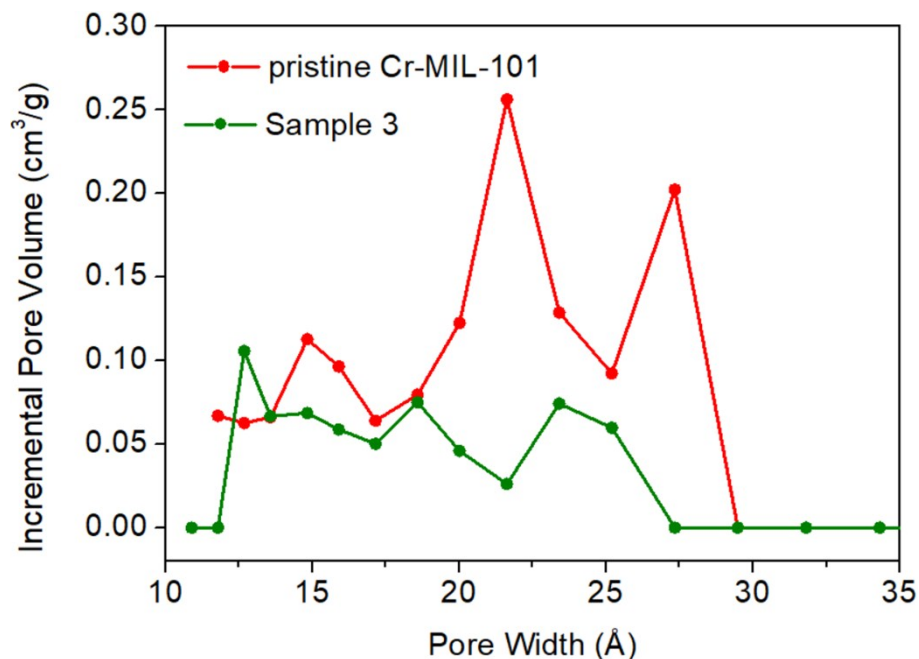


**Figure S3.** Pore size distribution of **Sample 3** in comparison with that of the pristine MIL-101(Cr). The total pore volume in **Sample 3** ( $\leq 272.71 \text{ \AA}$ ) is determined to be  $0.64595 \text{ cm}^3/\text{g}$ .

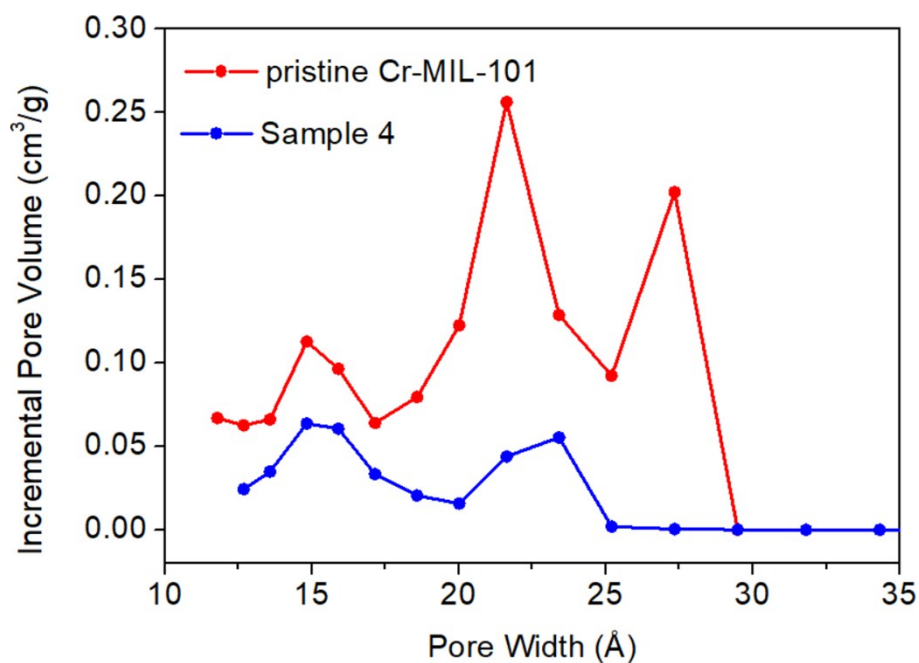


**Figure S4.** Pore size distribution of **Sample 4** in comparison with that of the pristine MIL-101(Cr). The total pore volume in **Sample 4** ( $\leq 272.71 \text{ \AA}$ ) is determined to be  $0.35535 \text{ cm}^3/\text{g}$ .

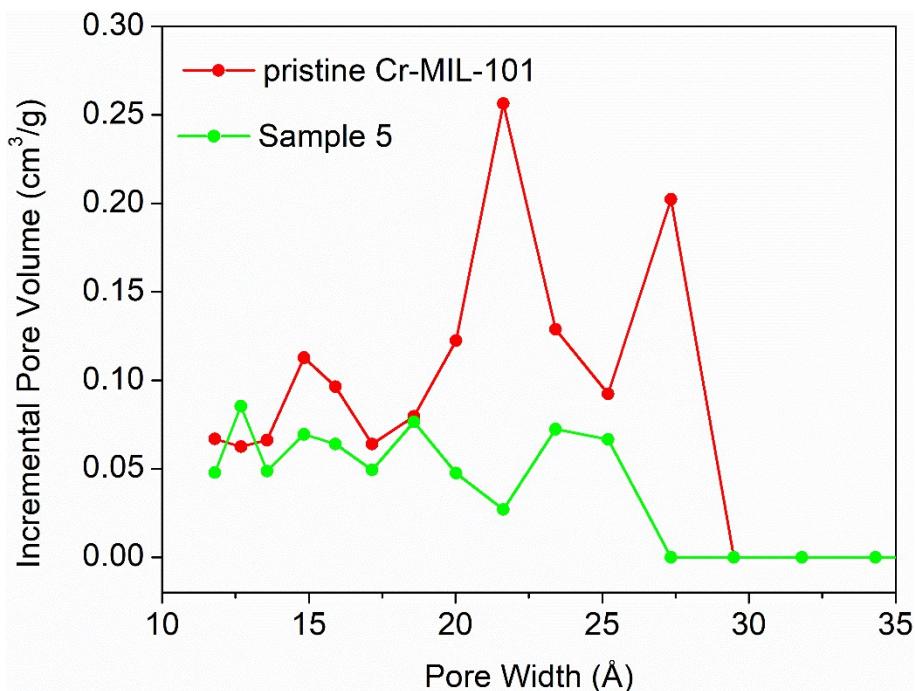


**Figure S5.** Pore size distribution of **Sample 5** in comparison with that of the pristine MIL-101(Cr). The total pore volume in **Sample 5** ( $\leq 272.71 \text{ \AA}$ ) is determined to be  $0.66322 \text{ cm}^3/\text{g}$ .

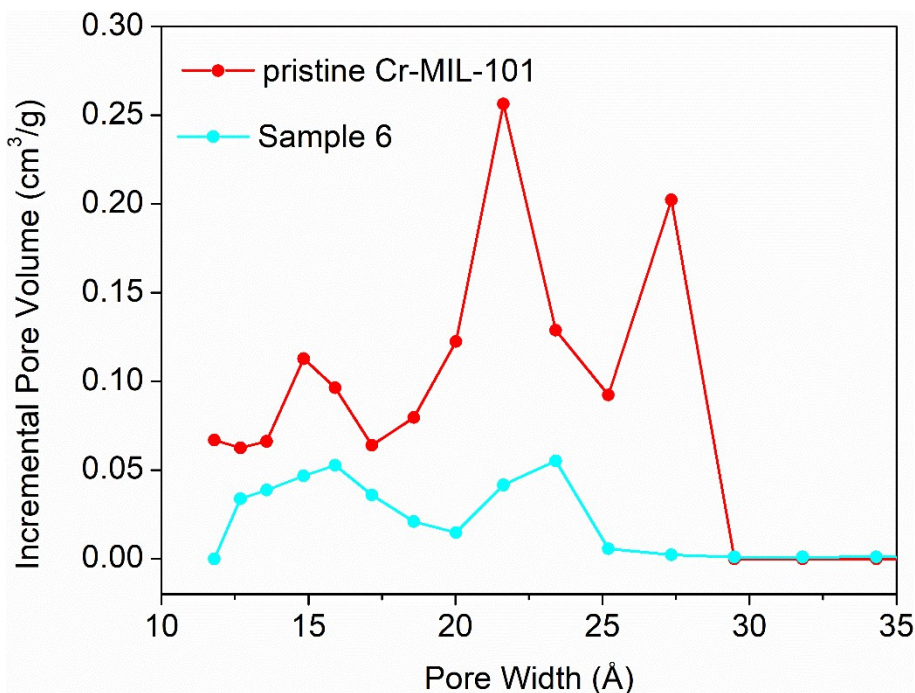


**Figure S6.** Pore size distribution of **Sample 6** in comparison with that of the pristine MIL-101(Cr). The total pore volume in **Sample 6** ( $\leq 216.60 \text{ \AA}$ ) is determined to be  $0.36741 \text{ cm}^3/\text{g}$ .

## Section 5. PXRD patterns of alkylamine-modified MIL-101(Cr)

The PXRD patterns of the samples were collected using a BRUKER D8-Focus Bragg-Brentano X-ray Powder Diffractometer equipped with a Cu sealed tube ( $\lambda = 1.54178 \text{ \AA}$ ) at 40 kV and 40 mA. The ranges of  $2\theta$  were all set to be 2-30 degrees.

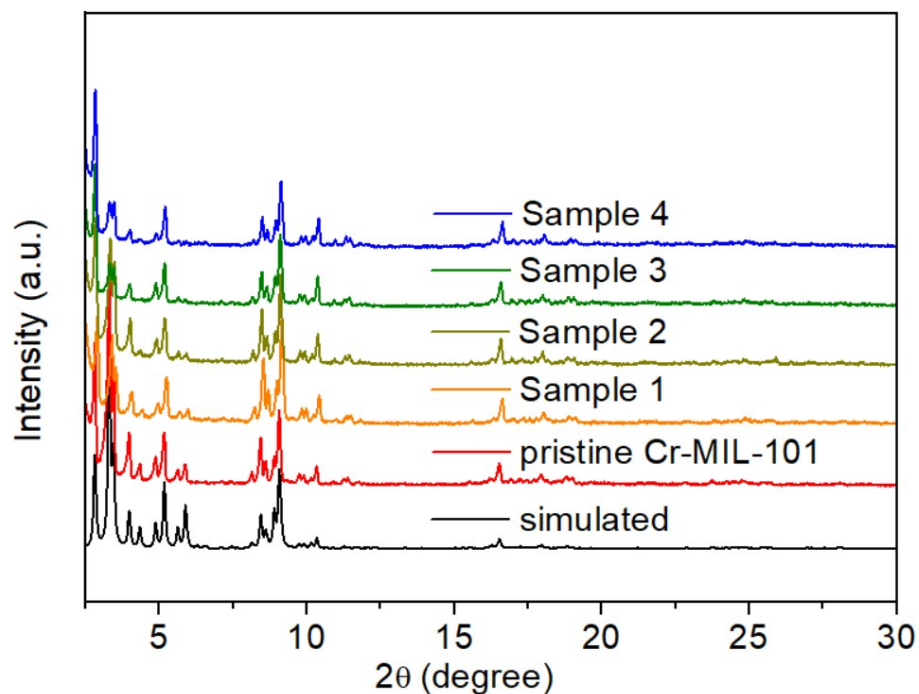


**Figure S7.** Comparison of the PXRD patterns of **Sample 1-4** with that of pristine MIL-101(Cr) and the simulated pattern.

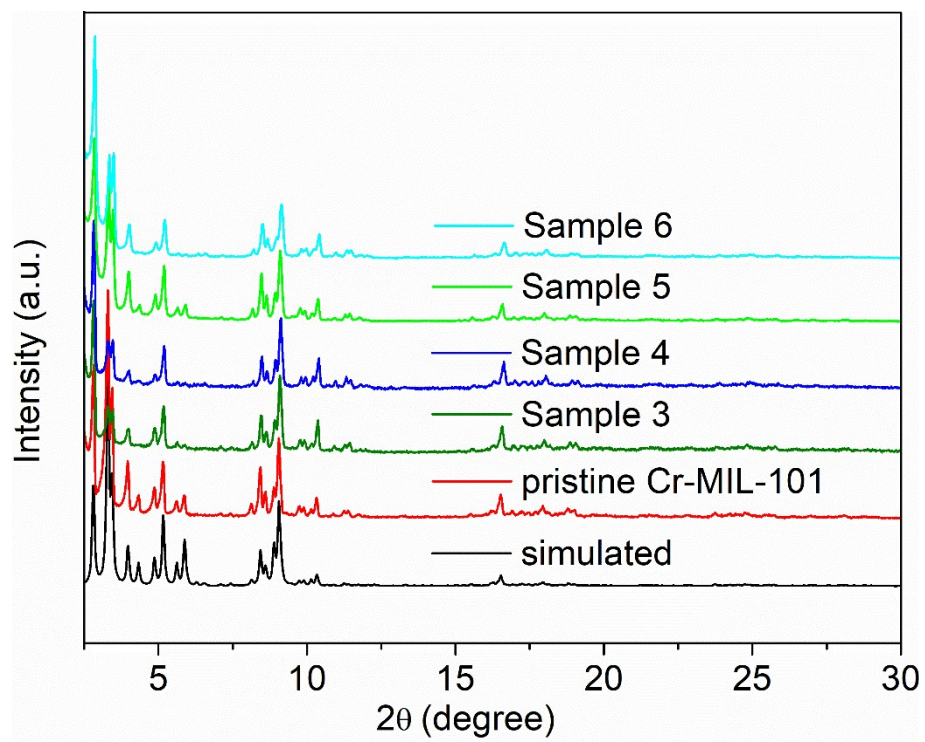


**Figure S8.** Comparison of the PXRD patterns of **Sample 3-6** with that of pristine MIL-101(Cr) and the simulated pattern.

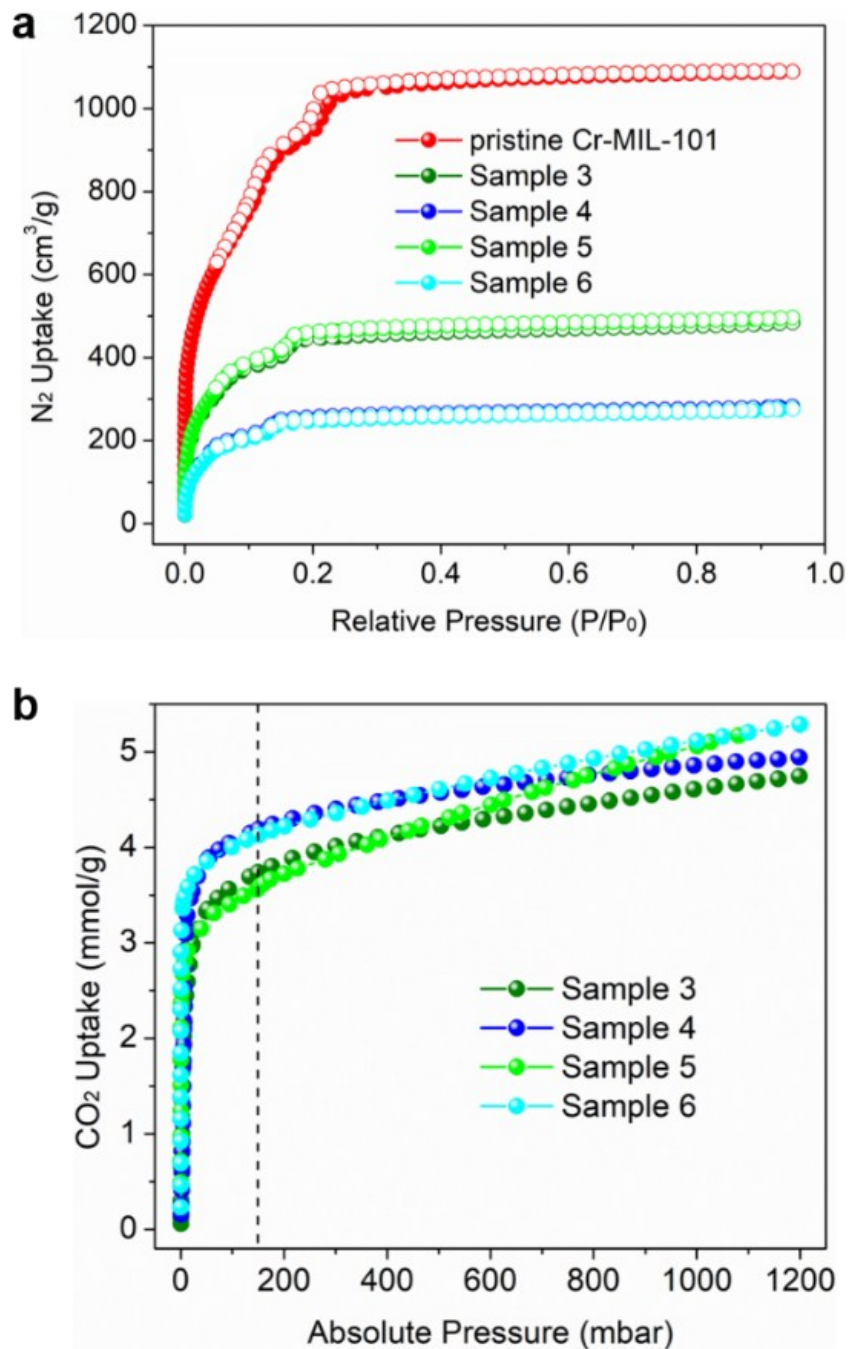
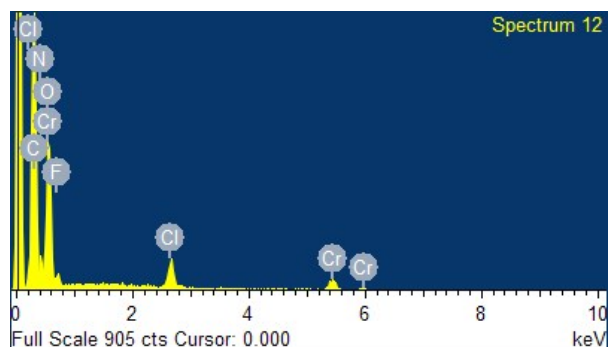


**Figure S9.** (a) N<sub>2</sub> uptakes at 77 K of **Sample 3-6** in comparison with that of the pristine MIL-101(Cr); (b) CO<sub>2</sub> uptakes at 25 °C of **Sample 3-6**. The dashed line represents an absolute pressure of 150 mbar.

## Section 6. EDX measurement of alkylamine-modified MIL-101(Cr)

The sample was first desiccated to remove moisture or solvent residues. After that, it was finely ground before being applied on a conductive tape which was adhered to the EDX sample holder. After the sample was placed into the SEM/EDX instrument, the inner pressure was decreased below  $10^{-6}$  torr before measurements were conducted. The scanning areas were all set to be approximately  $40 \times 40 \mu\text{m}^2$  to detect the element species.

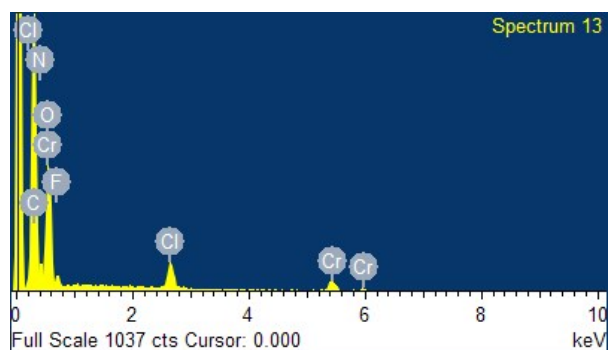
### 6.1. Sample 1



**Figure S10.** EDX spectrum of **Sample 1** (1st measurement).

**Table S1.** EDX data for **Sample 1** (1st measurement).

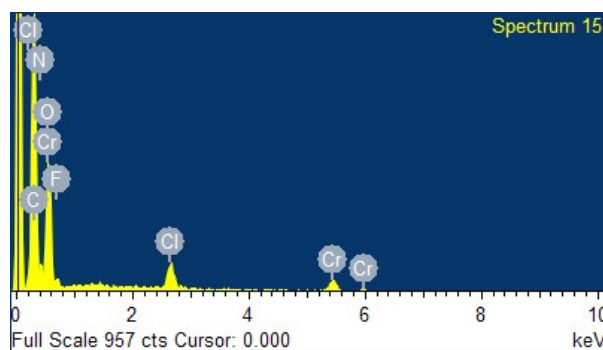
Element	Weight%	Atomic%
C K	40.05	56.55
N K	8.15	9.87
O K	19.55	20.72
F K	3.12	2.78
Cl K	3.83	1.83
Cr L	25.31	8.26
Totals	100.00	



**Figure S11.** EDX spectrum of **Sample 1** (2nd measurement).

**Table S2.** EDX data for **Sample 1** (2nd measurement).

Element	Weight%	Atomic%
C K	41.97	57.99
N K	8.10	9.60
O K	20.05	20.80
F K	2.69	2.35
Cl K	3.97	1.86
Cr L	23.22	7.41
Totals	100.00	

**Figure S12.** EDX spectrum of **Sample 1** (3rd measurement).**Table S3.** EDX data for **Sample 1** (3rd measurement).

Element	Weight%	Atomic%
C K	43.34	58.61
N K	7.73	8.96
O K	21.39	21.71
F K	2.80	2.39
Cl K	4.09	1.87
Cr L	20.65	6.45
Totals	100.00	

**Table S4.** Summary of the EDX data of **Sample 1**. F/Cr molar ratio = F Atomic% / Cr Atomic% = 2.51% / 7.37% = 0.340.

	F atomic%	Cr atomic%
1st measurement	2.78	8.26
2nd measurement	2.35	7.41
3rd measurement	2.39	6.45
Average	2.51	7.37

## 6.2. Sample 2

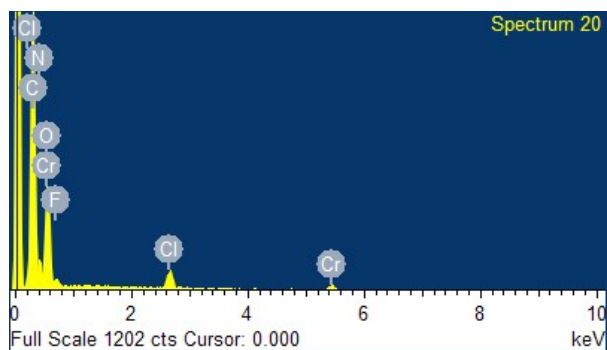


**Figure S13.** EDX spectrum of **Sample 2** (1st measurement).

**Table S5.** EDX data for **Sample 2** (1st measurement).

Element	Weight%	Atomic%
C K	43.37	58.72
N K	10.50	12.19
O K	18.30	18.60
F K	2.47	2.11
Cl K	3.03	1.39
Cr L	22.33	6.98
Totals	100.00	

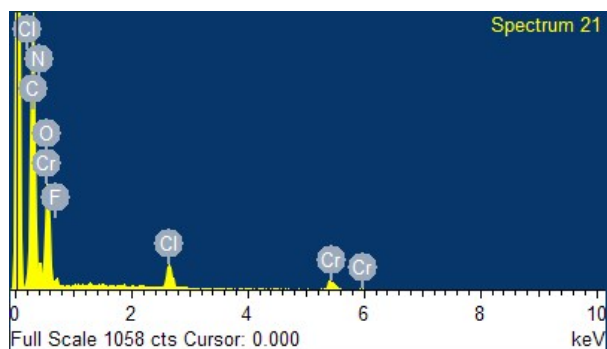


**Figure S14.** EDX spectrum of **Sample 2** (2nd measurement).

**Table S6.** EDX data for **Sample 2** (2nd measurement).

Element	Weight%	Atomic%
C K	46.61	60.60
N K	9.71	10.83
O K	20.56	20.07
F K	1.84	1.52
Cl K	4.23	1.86
Cr L	17.04	5.12
Totals	100.00	

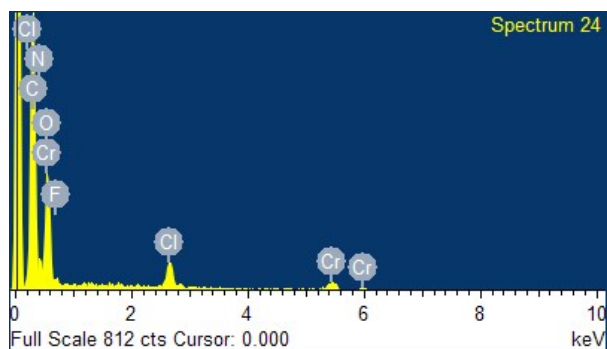


**Figure S15.** EDX spectrum of **Sample 2** (3rd measurement).

**Table S7.** EDX data for **Sample 2** (3rd measurement).

Element	Weight%	Atomic%
C K	46.11	60.02
N K	10.05	11.22
O K	20.59	20.12
F K	1.89	1.55
Cl K	4.69	2.07
Cr L	16.66	5.01
Totals	100.00	

**Table S8.** Summary of the EDX data of **Sample 2**.  $F/Cr$  molar ratio =  $F$  Atomic% /  $Cr$  Atomic% =  $1.73\% / 5.70\% = 0.304$ .

	F atomic%	Cr atomic%
1st measurement	2.11	6.98
2nd measurement	1.52	5.12
3rd measurement	1.55	5.01
Average	1.73	5.70

### 6.3. Sample 3

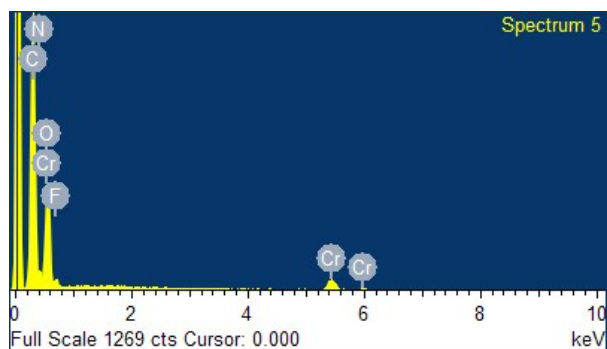


**Figure S16.** EDX spectrum of **Sample 3** (1st measurement).

**Table S9.** EDX data for **Sample 3** (1st measurement).

Element	Weight%	Atomic%
C K	44.70	59.80
N K	5.60	6.43
O K	23.89	23.99
F K	3.36	2.84
Cr L	22.46	6.94
Totals	100.00	

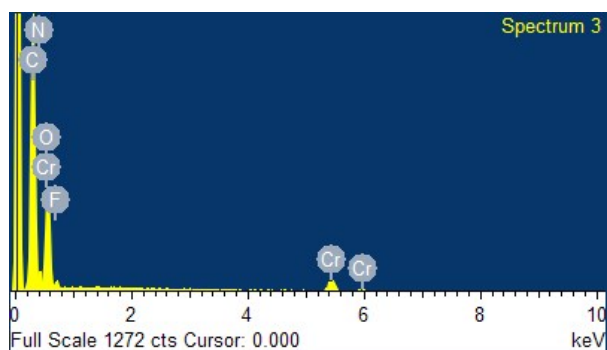


**Figure S17.** EDX spectrum of **Sample 3** (2nd measurement).

**Table S10.** EDX data for **Sample 3** (2nd measurement).

Element	Weight%	Atomic%
C K	42.88	59.28
N K	6.38	7.56
O K	21.04	21.84
F K	3.29	2.88
Cr L	26.42	8.44
Totals	100.00	

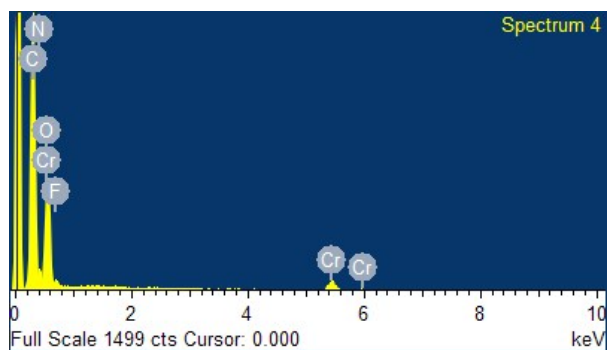


**Figure S18.** EDX spectrum of **Sample 3** (3rd measurement).

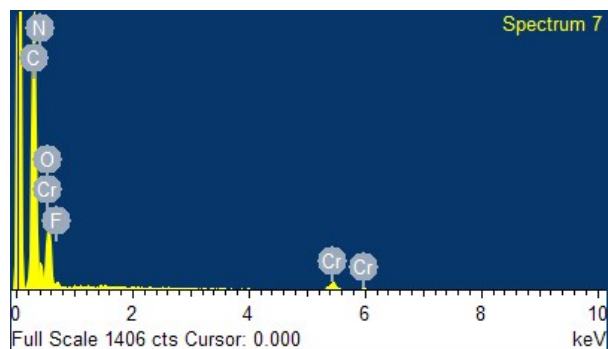
**Table S11.** EDX data for **Sample 3** (3rd measurement).

Element	Weight%	Atomic%
C K	43.43	59.86
N K	5.20	6.15
O K	22.47	23.25
F K	2.78	2.42
Cr L	26.13	8.32
Totals	100.00	

**Table S12.** Summary of the EDX data of **Sample 3**. F/Cr molar ratio = F Atomic% / Cr Atomic% = 2.45% / 7.89% = 0.310.

	F atomic%	Cr atomic%
1st measurement	2.06	6.92
2nd measurement	2.88	8.44
3rd measurement	2.42	8.32
Average	2.45	7.89

## 6.4. Sample 4

**Figure S19.** EDX spectrum of **Sample 4** (1st measurement).**Table S13.** EDX data for **Sample 4** (1st measurement).

Element	Weight%	Atomic%
C K	46.01	60.10
N K	13.38	14.99
O K	16.87	16.54
F K	2.29	1.89
Cr L	21.46	6.47
Totals	100.00	

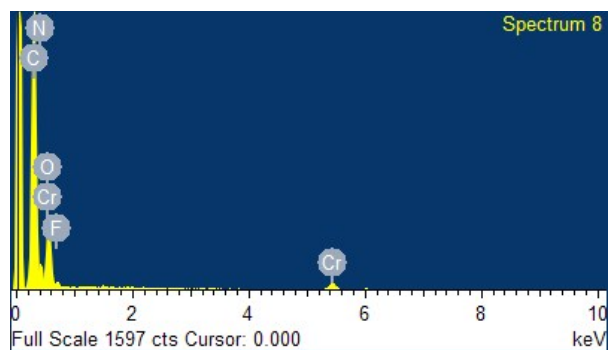


**Figure S20.** EDX spectrum of **Sample 4** (2nd measurement).

**Table S14.** EDX data for **Sample 4** (2nd measurement).

Element	Weight%	Atomic%
C K	46.83	60.93
N K	12.84	14.33
O K	17.05	16.65
F K	2.11	1.73
Cr L	21.18	6.36
Totals	100.00	

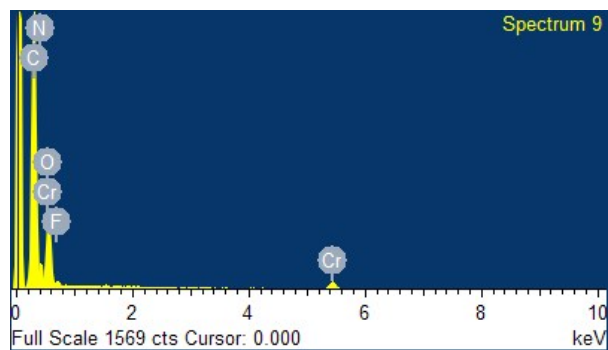


**Figure S21.** EDX spectrum of **Sample 4** (3rd measurement).

**Table S15.** EDX data for **Sample 4** (3rd measurement).

Element	Weight%	Atomic%
C K	45.04	59.73
N K	12.22	13.90
O K	17.33	17.25
F K	2.51	2.11
Cr L	22.90	7.02
Totals	100.00	

**Table S16.** Summary of the EDX data of **Sample 4**. F/Cr molar ratio = F Atomic% / Cr Atomic% = 1.91% / 6.62% = 0.288.

	F Atomic%	Cr Atomic%
1st measurement	1.89	6.47
2nd measurement	1.73	6.36
3rd measurement	2.11	7.02
Average	1.91	6.62

The F/Cr molar ratios of **Sample 1-4** are summarized in **Table S19**.

## Section 7. Elemental analysis of alkylamine-modified MIL-101(Cr)

Solid samples were sent to Atlantic Microlab, Inc. for elemental analysis.

**Table S17.** EA data of **Sample 1-4**. Each sample was measured twice.

Sample	C weight%	H weight%	N weight%	F weight%
Sample 1	37.35	5.61	8.93	1.68
	37.54	5.61	9.01	1.59
Sample 2	38.27	6.29	10.84	1.30
	38.15	6.18	10.75	1.21
Sample 3	40.22	5.77	11.78	1.28
	40.03	5.77	11.72	1.22
Sample 4	40.64	6.22	14.56	1.10
	40.46	6.16	14.49	1.07

**Table S18.** Average N weight%, average F weight% and the calculated N/F atomic ratios of **Sample 1-4**.

Sample	Average N weight%	Average F weight%	N/F atomic ratio
Sample 1	8.97	1.64	7.42
Sample 2	10.80	1.26	11.63
Sample 3	11.75	1.25	12.76
Sample 4	14.52	1.08	18.25

## Section 8. Molar ratios of the elements in alkylamine modified MIL-101(Cr)

The N/Cr molar ratios in alkylamine modified MIL-101(Cr) are obtained by multiplying the molar ratios of N/F and F/Cr in each sample.

**Table S19.** Summary of the N/F and F/Cr molar ratios of **Sample 1-4**, and their consequent N/Cr molar ratios.

Sample	n(N)/n(F) <sup>a</sup>	n(F)/n(Cr) <sup>b</sup>	n(N)/n(Cr)	n(alkylamine)/n(Cr)
Sample 1	7.42	0.34	2.52	0.84
Sample 2	11.63	0.30	3.49	0.87
Sample 3	12.76	0.31	3.96	1.32
Sample 4	18.25	0.29	5.29	1.32

<sup>a</sup>. n(N)/n(F) data are collected by EA. <sup>b</sup>. n(F)/n(Cr) data are collected by EDX.

## Section 9. Quantitative analysis of the organic components in alkylamine-modified MIL-101(Cr) using NMR

10 mg activated alkylamine-modified MIL-101(Cr) sample was added to a solution prepared from 200  $\mu\text{L}$  40% w/w NaOD solution in  $\text{D}_2\text{O}$  (99.5%) and 1200  $\mu\text{L}$   $\text{D}_2\text{O}$  for decomposition. After 24 h, the suspension became clear pale green solution, which was analyzed using NMR spectroscopy for the molar ratio between BDC and TAEA in the sample.

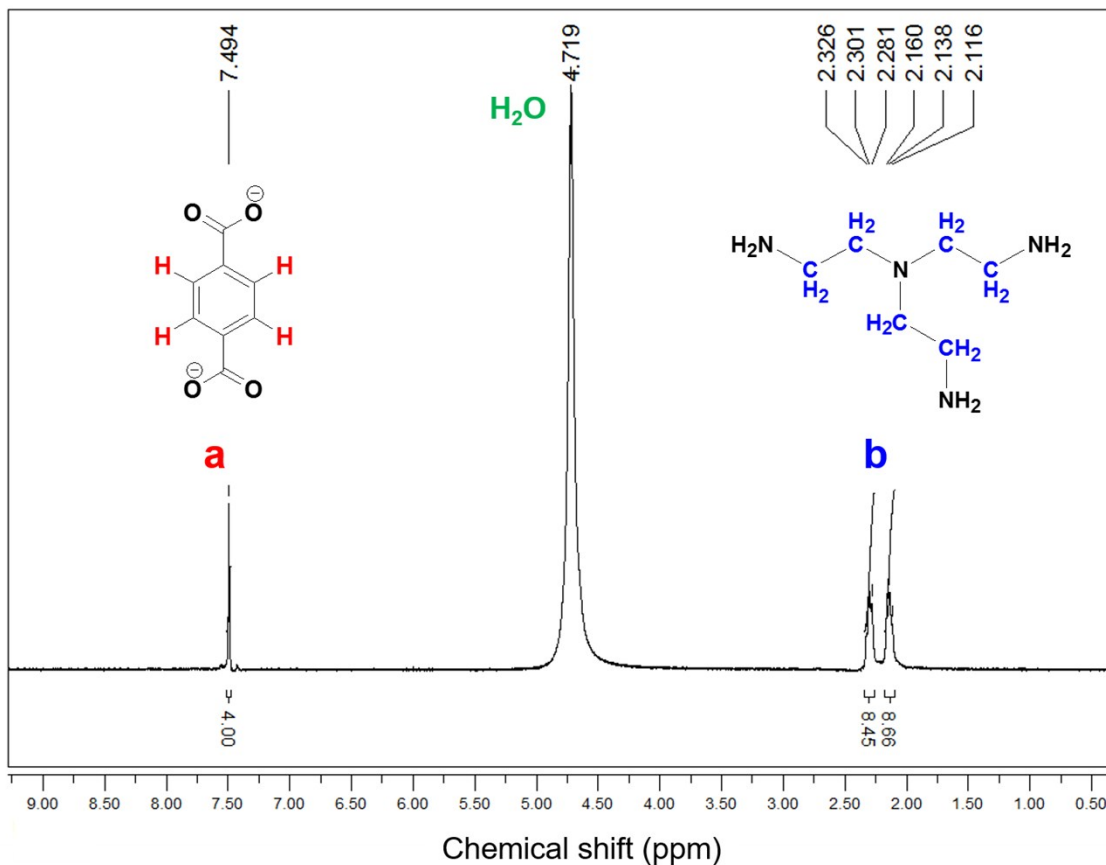


**Figure S22.** NMR spectrum of the decomposed **Sample 4** in a NaOD solution in  $\text{D}_2\text{O}$ .

The molar ratio between alkylamine and Cr in **Sample 4** was further confirmed by the NMR spectrum of the degraded **Sample 4** in NaOD/ $\text{D}_2\text{O}$  solution (**Figure S22**). The protons on BDC and TAEA were integrated to be 4 and 17.11, respectively. Therefore,  $n(\text{TAEA})/n(\text{BDC}) = (17.11/12)/(4/4) = 1.43/1$ . Since in MIL-101(Cr),  $n(\text{Cr})/n(\text{BDC}) = 1/1$ , it is reasonable to arrive at the conclusion that in **Sample 4**,  $n(\text{TAEA})/n(\text{Cr}) = 1.43/1$ . This result is comparable to the value (1.32) obtained by EDX and EA.

## Section 10. TGA measurement of alkylamine-modified MIL-101(Cr)

Sample 4 (around 10 mg) was placed in an aluminum pan, and kept under helium at 30 °C for 15 min to remove solvent residues. After that, the TGA measurement was initiated with the increasing rate of temperature set as 5 °C/min. The emitted gas species were detected using an OmniStar ThermoStar GSD320 Gas Analysis System.

The experimental results show two steps of mass loss as the temperature increases. The first step is associated with the desorption of CO<sub>2</sub> (adsorbed during the sample transfer from the BET tube to the TGA instrument), as indicated by the mass peak of 44 in the mass spectrum. The second step is correlated with the decomposition of TAEA, which is suggested by the mass peak of 30 (one characteristic peak of TAEA).

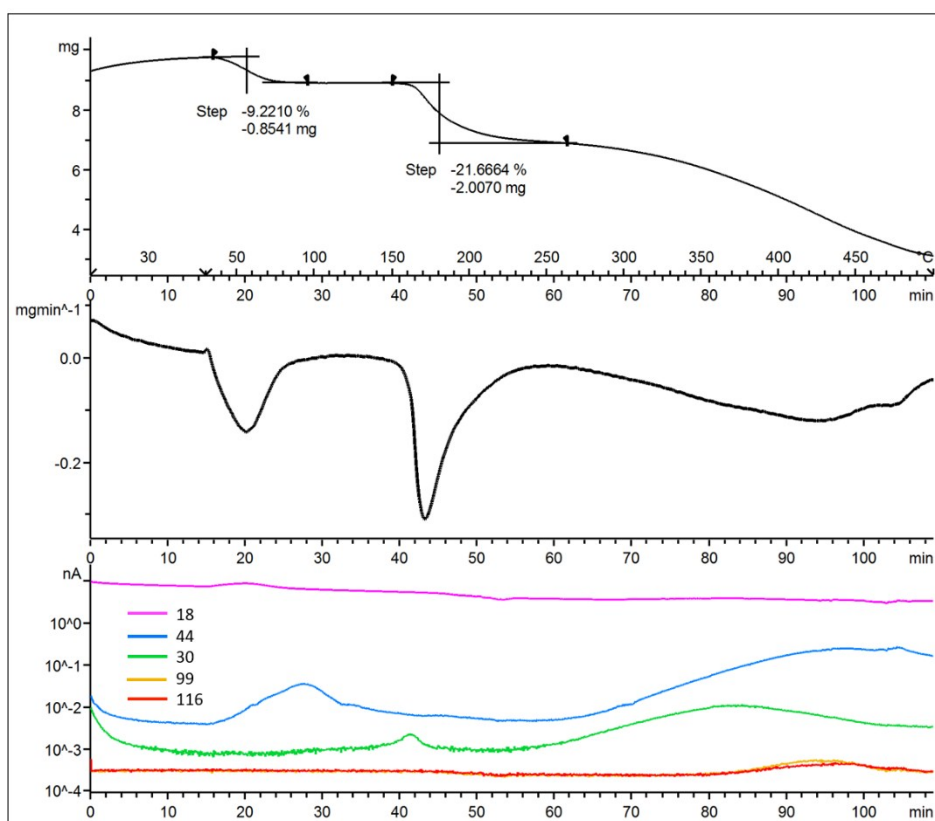


**Figure S23.** The TGA curve (upper), the first derivative of the TGA curve (middle) and the mass spectrum of the released species (lower) of **Sample 4** as the temperature rises from 30 °C to 500 °C.

## Section 11. Virial fitting of the CO<sub>2</sub> adsorption isotherms of Sample 4

A Virial-type expression of comprising the temperature-independent parameters  $a_i$  and  $b_j$  was employed to calculate the enthalpies of adsorption for CO<sub>2</sub> (at 273 K and 298 K) on Sample 4. In each case, the data were fitted use equation:

$$\ln P = \ln N + 1/T \sum_{i=0}^m a_i N_i + \sum_{j=0}^n b_j N_j$$

Here,  $P$  is the pressure expressed in mmHg,  $N$  is the amount absorbed in mmol/g,  $T$  is the temperature in K,  $a_i$  and  $b_j$  are Virial coefficients, and  $m$ ,  $n$  represent the number of coefficients required to adequately describe the isotherms ( $m$  and  $n$  were gradually increased till the contribution of extra added  $a$  and  $b$  coefficients was deemed to be statistically insignificant towards the overall fit. The average value of the squared deviations from the experimental values was minimized). The values of the Virial coefficients  $a_0$  through  $a_m$  were then used to calculate the isosteric heat of absorption using the following expression:

$$Q_{st} = -R \sum_{i=0}^m a_i N_i$$

$-Q_{st}$  is the coverage-dependent isosteric heat of adsorption and  $R$  is the universal gas constant. The  $-Q_{st}$  for Sample 4 was determined with the adsorption data measured in the pressure range from 0-1 bar at 273 K and 303 K.

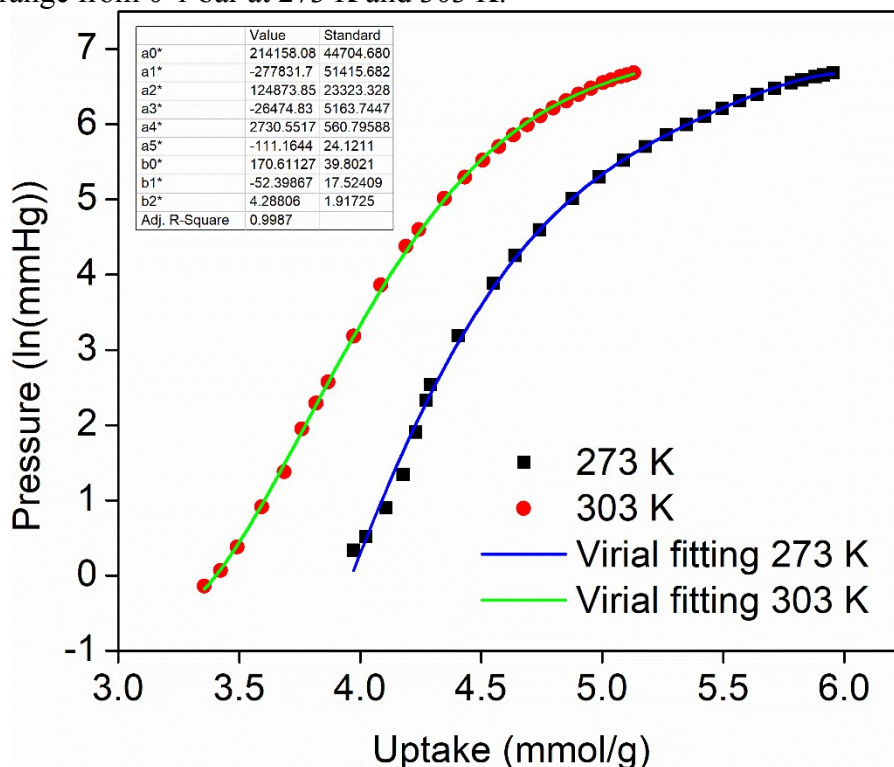


**Figure S24.** The TGA curve (upper), the first derivative of the TGA curve (middle) and the mass spectrum of the released species (lower) of **Sample 4** as the temperature rises from 30 °C to 500 °C.

## Section 12. Dynamic column breakthrough experiments

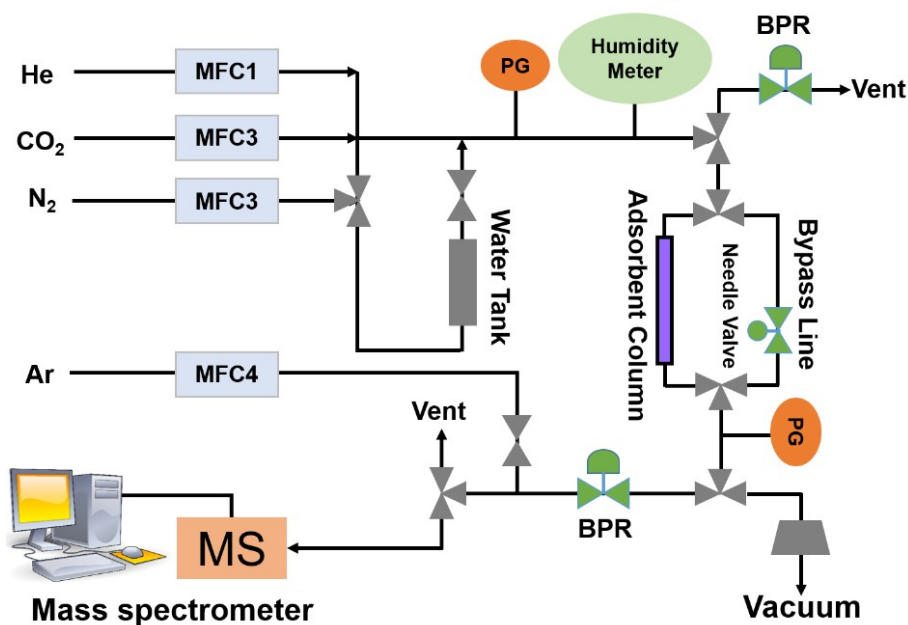


**Figure S25.** The layout of the home-built breakthrough equipment. MFC, PG, BPR are abbreviations for micro flow controller, pressure gauge, and back pressure regulator, respectively.

## Section 13. Selectivity calculation based on breakthrough experiment data

The simplified model for breakthrough related calculations is presented in **Figure S26**.

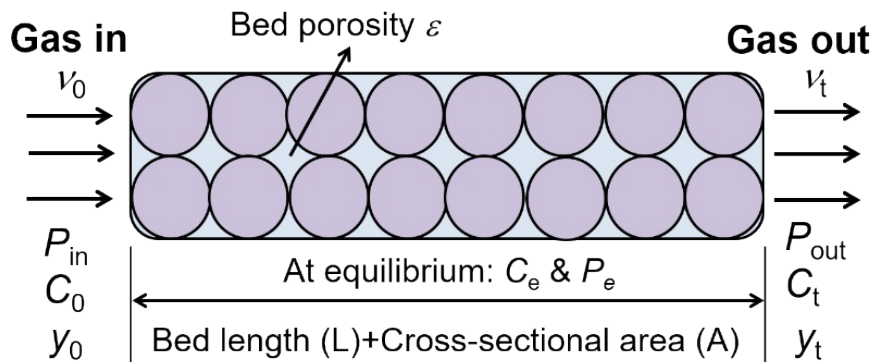


**Figure S26.** Model and parameters for adsorptive separation calculations.

From the mass balance across the whole packed column ( $In - Out = Accumulation$ ), the following equations can be obtained:

$$\varepsilon v_0 C_0 A t_c - \int_0^{t_c} \varepsilon v_t C_t A dt = LA \varepsilon C_e + LA(1 - \varepsilon) q_e \quad \text{(Equation 1)}$$

$$C_0 = \frac{P_{in}}{R \times T}; C_t = \frac{P_{out}}{R \times T} \quad \text{(Equation 2)}$$

Where  $\varepsilon$  is the bed porosity,  $v_0$  is the interstitial feed gas velocity ( $\text{cm s}^{-1}$ ),  $C_0$  is the inlet gas concentration ( $\text{mmol cm}^{-3}$ ),  $A$  is the cross sectional area of column ( $\text{cm}^2$ ),  $t_c$  is the elution time (s),  $v_t$  is the interstitial outlet gas velocity ( $\text{cm s}^{-1}$ ),  $C_t$  is the outlet gas concentration ( $\text{mmol cm}^{-3}$ ),  $C_e$  is the average gas concentration at adsorption equilibrium ( $\text{mmol cm}^{-3}$ ),  $P_{in}$  and  $P_{out}$ , and  $P_e$  are the inlet (upstream), outlet (downstream), and equilibrium pressure (assume an average value of upstream and downstream pressure), respectively,  $L$  is the column length (cm),  $r_p$  is the radius of crystal size;  $q_e$  is the equilibrium concentration of adsorbate in the adsorbent ( $\text{mmol cm}^{-3}$ ).<sup>2</sup>

According to Darcy's Law, the cross-column pressure drop is related to the viscosity of gas phase ( $\mu$ ), interstitial gas velocity and column length:

$$\frac{\Delta P}{L} = \frac{150}{4r_p^2} \left( \frac{1 - \varepsilon}{\varepsilon} \right)^2 \mu v_t \quad \text{(Equation 3)}$$

Since the product of viscosity of gas phase ( $\mu$ ), interstitial gas velocity ( $v_t$ ) can be deemed as a constant, it is reasonable to assume the equilibrium pressure ( $P_e$ ) equals to:

$$P_e \approx \frac{P_{in} + P_{out}}{2}; C_e \approx \frac{P_{in} + P_{out}}{2R \times T} \quad \text{(Equation 4)}$$

After rearrangement, the **Equation 1** for mean residence time  $\bar{t}$  is obtained:

$$\int_0^{t_c} \left( 1 - \frac{v_t C_t}{v_0 C_0} \right) dt = \bar{t} = \frac{L}{v_0} \left[ \frac{P_{in} + P_{out}}{2P_{in}} + \frac{1 - \varepsilon}{\varepsilon} \left( \frac{q_e}{C_0} \right) \right] \quad \text{(Equation 5)}$$

For each component,  $y_0$  and  $y_t$  represent the inlet and outlet molar fraction:

$$y_0 = y_t^\infty; v_0 = v_t^\infty \times \frac{P_{out}}{P_{in}}; \frac{v_t}{v_0} = \frac{v_t^\infty}{v_t^\infty} \times \frac{P_{in}}{P_{out}}$$

$$\frac{C_t}{C_0} = \left( \frac{y_t P_{out}}{R \times T} \right) / \left( \frac{y_0 P_{in}}{R \times T} \right) = \frac{y_t}{y_0} \times \frac{P_{out}}{P_{in}};$$

$$\frac{C_t}{C_0} \times \frac{v_t}{v_0} = \frac{v_t y_t}{v_t^\infty y_t^\infty} \quad \text{(Equation 6)}$$

The following equation can be obtained:

$$\int_0^{t_c} \left( 1 - \frac{v_t y_t}{v_t^\infty y_t^\infty} \right) dt = \bar{t} = \frac{L}{v_0} \left[ \frac{P_{in} + P_{out}}{2P_{in}} + \frac{1 - \varepsilon}{\varepsilon} \left( \frac{q_e}{C_0} \right) \right] \quad \text{(Equation 7)}$$

The mean residence time obtained from the experimentally measured breakthrough responses after subtracting blank residence time (dead volume calibration) can be used to calculate  $q_e/C_0$ . The adsorption selectivity ( $S_{ads}$ ) at equilibrium pressure can be calculated:

$$S_{ads} = \frac{(q_e/C_0)_{CO_2}}{(q_e/C_0)_{N_2}} \quad \text{(Equation 8)}$$

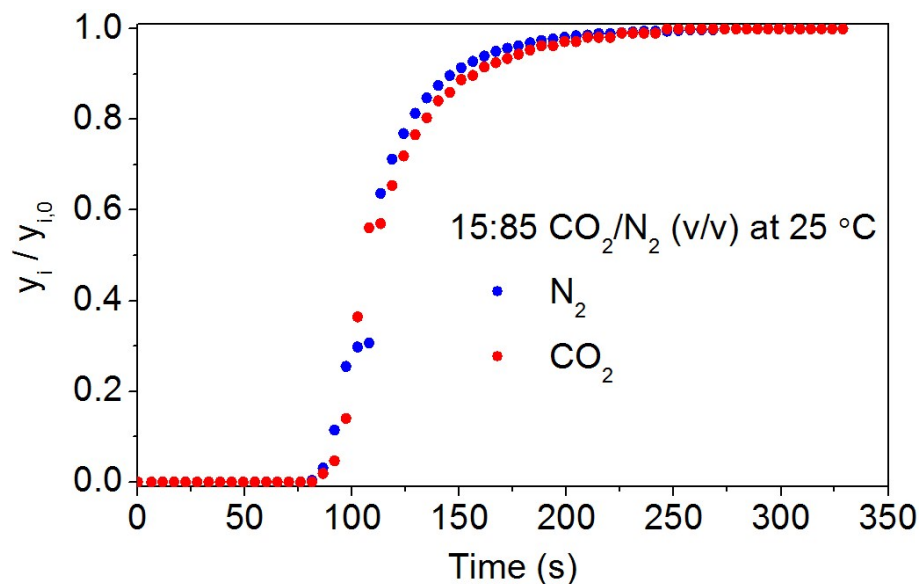


**Figure S27.** Breakthrough curves of an empty column for dead volume calibration at 25 °C. The gas flow is a  $15 \pm 1:85 \pm 1$  CO<sub>2</sub>/N<sub>2</sub> (v/v) flow at 25 °C with an inlet pressure of 1.2 bar and an outlet pressure of 1 bar.  $y_i$  and  $y_{i,0}$  are the molar fractions of a gas species at the inlet and outlet, respectively.

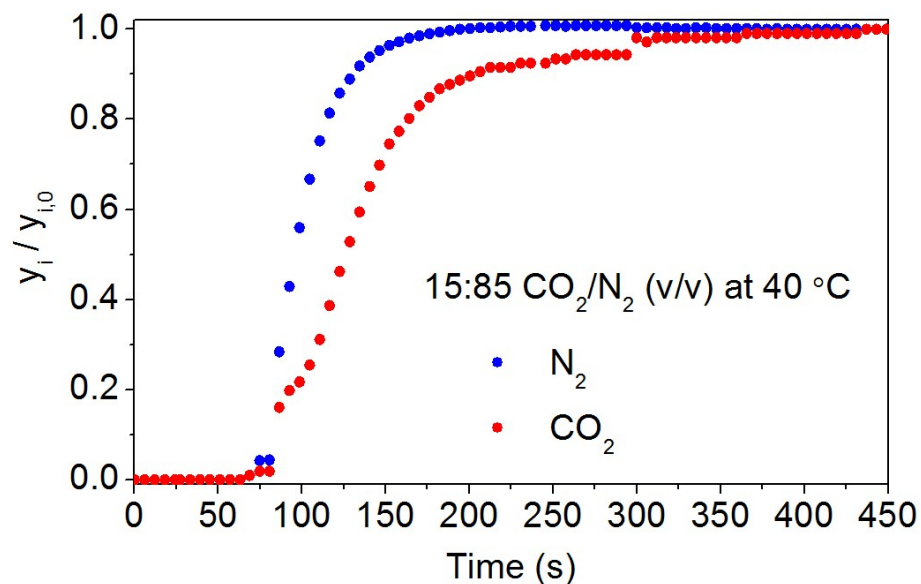


**Figure S28.** Breakthrough curves of an empty column for dead volume calibration at 40 °C. The gas flow is a  $15 \pm 1:85 \pm 1$  CO<sub>2</sub>/N<sub>2</sub> (v/v) flow at 40 °C with an inlet pressure of 1.2 bar and an outlet pressure of 1 bar.  $y_i$  and  $y_{i,0}$  are the molar fractions of a gas species at the inlet and outlet, respectively.

## Section 14. Rationalization of alkylamine incorporation from a chemical potential perspective

Assume there are two MIL-101(Cr) samples with equal mass. Alkylamine incorporation are conducted with these two samples using CH and DCM as the solvent, respectively. For comparison, we suppose there are equal amounts of a certain alkylamine integrated into these two samples. Thus, the chemical potentials of alkylamine in the both MOFs are the same, denoted as  $\mu_{\text{MOF}}$ . When a thermodynamic equilibrium is reached between the solution phase and the MOF phase, the chemical potential of alkylamine in the solution  $\mu_{\text{c, solvent}}$  should be equal to that in the MOF  $\mu_{\text{MOF}}$ .

$$\mu_{\text{c, CH}} = \mu_{\text{c, CH}}^{\circ} + RT \ln(c_{\text{CH}}/c^{\circ}) = \mu_{\text{MOF}} \quad \text{(Equation 9)}$$

$$\mu_{\text{c, DCM}} = \mu_{\text{c, DCM}}^{\circ} + RT \ln(c_{\text{DCM}}/c^{\circ}) = \mu_{\text{MOF}} \quad \text{(Equation 10)}$$

$\mu_{\text{c, solvent}}^{\circ}$  is the standard chemical potential of alkylamine in a solvent.  $c_{\text{solvent}}$  is the molar concentration of alkylamine in a solvent.  $c^{\circ}$  is the standard molar concentration.<sup>3</sup>

Therefore we have,

$$\mu_{\text{c, CH}}^{\circ} + RT^{\circ} \ln(c_{\text{CH}}/c^{\circ}) = \mu_{\text{c, DCM}}^{\circ} + RT^{\circ} \ln(c_{\text{DCM}}/c^{\circ})$$

So we have,

$$c_{\text{CH}}/c_{\text{DCM}} = \exp[(\mu_{\text{c, DCM}}^{\circ} - \mu_{\text{c, CH}}^{\circ})/RT] \quad \text{(Equation 11)}$$

Since  $\mu_{\text{c, DCM}}^{\circ} - \mu_{\text{c, CH}}^{\circ} < 0$ ,

Thus,  $c_{\text{CH}}/c_{\text{DCM}} < 1$ .

This indicates that the  $c_{\text{CH}}$  required to incorporate a certain amount of alkylamine into MIL-101(Cr) is less than  $c_{\text{DCM}}$ . This conclusion is based upon the assumption that an equal amount of alkylamine is integrated into the two MOFs, respectively, so it is reasonable to deduce that a higher percentage of alkylamine would be incorporated into the framework in the case of CH than that in DCM if the initial  $c_{\text{solvent}}$  are the same. This reasoning from the perspective of chemical potential suggests that using the less polar CH to disperse alkylamine is more favorable to drive more alkylamine molecules into the MOF.

## Section 15. CO<sub>2</sub> isotherms of alkylamine-modified MIL-101(Cr)

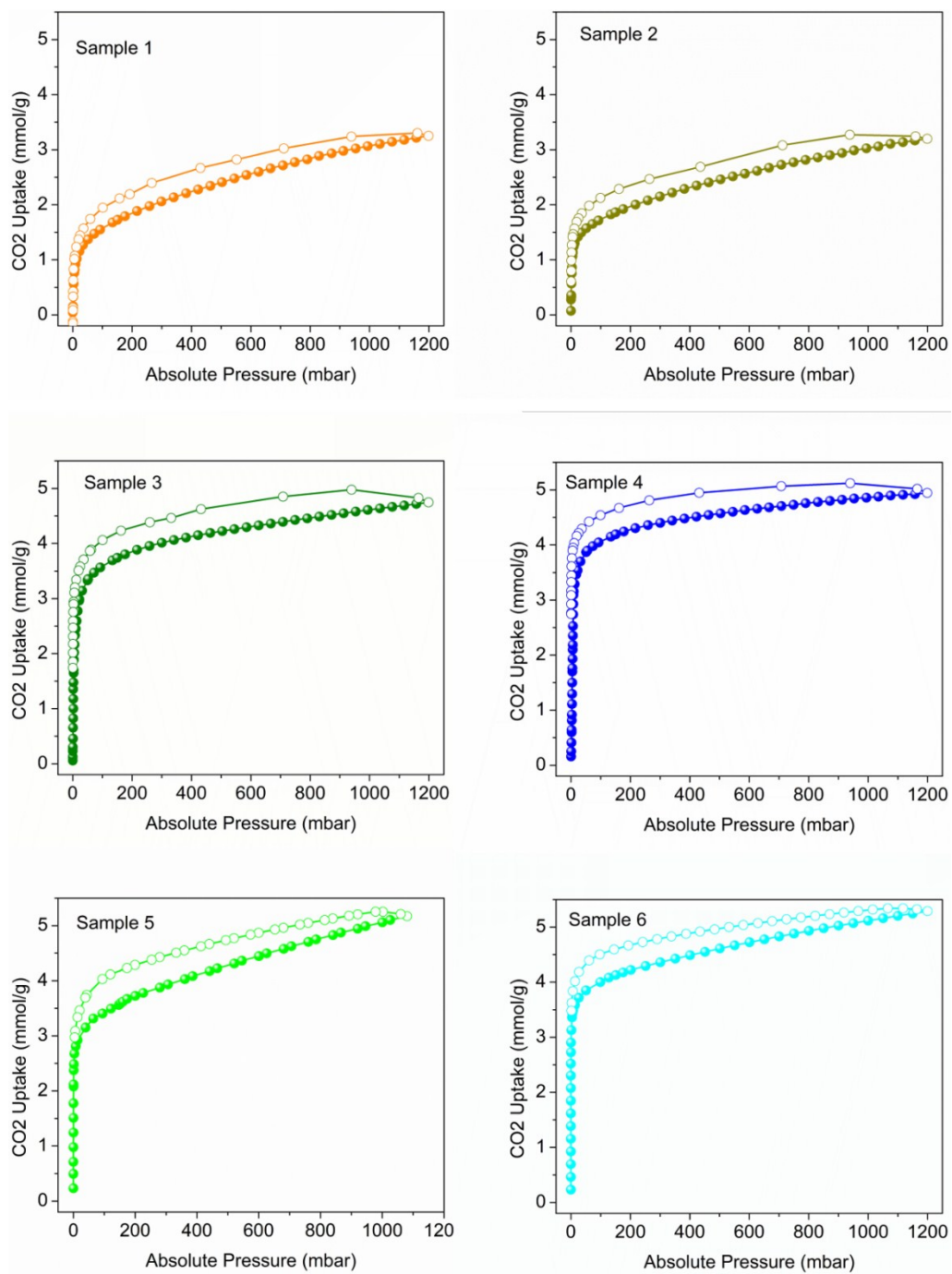


**Figure S29.** CO<sub>2</sub> sorption isotherms (solid, adsorption; hollow, desorption) of Sample 1-6.

## References

1. G. Férey, C. Mellot-Draznieks, C. Serre, F. Millange, J. Dutour, S. Surblé and I. Margiolaki, *Science*, 2005, **309**, 2040.
2. (a) S. Farooq and D. M. Ruthven, *AIChE J.*, 1991, **37**, 299; (b) A. Malek and S. Farooq, *AIChE J.*, 1997, **43**, 761; (c) Z. Hu, M. Khurana, Y. H. Seah, M. Zhang, Z. Guo and D. Zhao, *Chem. Eng. Sci.*, 2015, **124**, 61.
3. (a) J. S. Winn, *Physical Chemistry*. HarperCollins College Publishers: 1995; (b) D. A. McQuarrie and J. D. Simon, *Physical Chemistry: A Molecular Approach*. University Science Books: 1997.